# An underdetermined convolutional blind separation algorithm for time-frequency overlapped wireless communication signals with unknown source number

**Hao Ma**
Army Engineering University of PLA https://orcid.org/0000-0002-4915-5893
**Xiang Zheng** ( zhengxiang@aeu.edu.cn )
Army Engineering University of PLA
**Xinrong Wu**
Army Engineering University of PLA
**Lu Yu**
Army Engineering University of PLA
**Yu Zhang**
Army Engineering University of PLA

**Research**

**Keywords:** underdetermined blind separation, TF overlapped signals, TF soft mask, KDE algorithm, contribution degree function

**Posted Date:** February 15th, 2022

**DOI:** https://doi.org/10.21203/rs.3.rs-1348322/v1

RESEARCH

# An underdetermined convolutional blind separation algorithm for time-frequency overlapped wireless communication signals with unknown source number

Hao Ma, Xiang Zheng*, Xinrong Wu, Lu Yu and Yu Zhang

*Correspondence:
zhengxiang@aeu.edu.cn
School of Communication Engineering, Army Engineering University, Nanjing, China
Full list of author information is available at the end of the article

**Abstract**

It has been challenging to separate the time-frequency (TF) overlapped wireless communication signals with unknown number of sources in underdetermined cases. To address this issue, a novel blind separation strategy based on a TF soft mask is proposed in this paper. Based on the clustering property of the signals in the sparse domain, the angular probability density distribution is obtained by the kernel density estimation (KDE) algorithm, and then the number of source signals is identified by detecting the peak points of the distribution. Afterwards, the contribution degree function is designed according to the cosine distance to calculate the contribution degrees of the source signals in the mixed signals. The separation of the TF overlapped signals is achieved by constructing a soft mask matrix based on the contribution degrees. In this paper, the simulations are performed with digital signals of the same modulation and different modulation respectively. The results show that the proposed algorithm has better anti-aliasing and anti-noise performance than the benchmark algorithms.

**Keywords:** underdetermined blind separation; TF overlapped signals; TF soft mask; KDE algorithm; contribution degree function

## 1 Introduction

Blind source separation (BSS), defined as the task of separating the source signals from the observed signals when the source signals and the mixing mode are not known exactly, enables the separation of the mixed signals and the extraction of the source signals with information data. As a front-end technology in the field of signal processing, the BSS is of great importance in communication anti-jamming and improving spectrum utilization [1]. Unfortunately, the classical independent component analysis (ICA) and many extended algorithms [2-4] are based on the main assumption that the number of observed signals is greater than or equal to the number of source signals, which cannot realize the blind signal separation in underdetermined cases [5]. In practical communication scenarios, the number of observed signals is usually less than the number of source signals on account of system cost or environmental constraints, thus the study of underdetermined blind source separation (UBSS) is of more practical significance. At present, the main approach to tackle the issue of UBSS is based on sparse component analysis (SCA) [6].

The main strategy of the SCA method is solving the UBSS by exploiting the sparsity of the source signal or sparsity in the transform domain. The traditional SCA algorithm mainly consists of the two-stage method and the TF masking method. The two-stage method first estimates the mixing matrix and then uses signal sparsity to recover the source signal. Zhen [7] utilized the sparse coding technique to discover the 1-D subspace from the set of TF points, then estimated the mixing matrix by grouping vectors in the subspace through hierarchical clustering, and finally used the least-squares method to achieve source signal recovery; Fang [8] firstly estimated the mixing matrix based on the hyperplane normal vector clustering algorithm, and then used the classical algorithm called orthogonal matching pursuit in compressed sensing to realize the separation of the chirp radar mixed signals; Fu [9] realized the recovery of the source signal using a new subspace complementary matching pursuit algorithm. The algorithm reduced the computational complexity by selecting multiple atoms per iteration and also used L2 parametric minimization instead of L0 parametric minimization in order to improve the recovery accuracy. The other is the TF masking method, i. e., the source signal is separated by designing a TF mask matrix. Yu [10] firstly detected the peak energy point of the mixed signals, and then calculated the cosine distance between all energy points and the peak energy point, afterward obtained the binary mask based on a threshold to realize the reconstruction of the vibration signal; Cobos [11] proposed a maximum a posteriori decision criterion to design a binary mask matrix for the separation of mixed speech signals; Kumar [12] first detected the active single-source points by calculating the mixing ratio, and then found the cluster centers by a dynamic routing algorithm as a way to design a binary mask. The above algorithms have achieved satisfactory performance in the fields of modality recognition and speech separation, etc. However, in the wireless communication scenarios, the signals are overlapped in both time and frequency domains. In such cases, the two-stage method could not guarantee the estimation accuracy of the mixing matrix and the performance of the source signal recovery, while reconstructing the source signals through the TF binary mask will bring certain distortions [13-15]. Obviously, for the communication mixed signals with TF aliasing, better separation performance can be obtained by reasonably estimating the TF soft mask to reconstruct the source signals [16].

Under the framework of the TF masking method, we propose a novel underdetermined convolutional hybrid UBSS algorithm for TF overlapped communication signals with unknown number of sources. Firstly, the observed signals are converted to the sparse domain to obtain the linear clustering characteristic. Consequently, the effects of multipath and time delay are eliminated by calculating short-time spectral power; Secondly, the short-time spectral power ratio of the observed signals is converted into the angular distribution, and the number of source signals can be estimated through the KDE algorithm; Finally, the contribution degree of the source signal in the observed signal is obtained by the designed contribution degree function. The TF soft mask is constructed based on the contribution degree, which is employed to the separate the mixed signals. Simulations show that, compared with the benchmark algorithms, the algorithm proposed in this paper has better anti-aliasing and anti-noise performance.

The rest of this paper is structured as follows. The problem statement is given in Section 2, which includes the introduction of the effect on separation based

on the traditional SCA methods caused by TF aliasing. Subsequently, Section 3 describes the process of the algorithm in detail, which mainly consists of two parts: source number estimation and source signal recovery. Afterwards, the separation performance of this algorithm is tested by the simulations in Section 4. Lastly, the conclusions are drawn in Section 5.

## 2 Problem statement

In the wireless communication propagation model, multipath and time delay of signals are inevitable, which can be modeled as the convolutive mixture of the source signals [17]. Without considering the noise, the mathematical expression of the convolutional mixture model can be expressed as

$$\boldsymbol{x}(t) = \sum_{q=\mathbf{1}}^{Q} \boldsymbol{A}_q \boldsymbol{s}(t) \tag{1}$$

where $\boldsymbol{s}(t)$ represents the source signal; $\boldsymbol{x}(t)$ indicates the received mixed signal; $Q$ is the number of wireless propagation paths; $\boldsymbol{A}_q$ denotes the mixing matrix corresponding to the $q$th path. Considering the effect of time delay, $\boldsymbol{A}_q$ can be expressed as:

$$\boldsymbol{A}_q = \begin{bmatrix} a_{11}^q \delta(t-\tau_{11}^q) & a_{12}^q \delta(t-\tau_{12}^q) & \cdots & a_{1n}^q \delta(t-\tau_{1n}^q) \\ a_{21}^q \delta(t-\tau_{21}^q) & a_{22}^q \delta(t-\tau_{22}^q) & \cdots & a_{2n}^q \delta(t-\tau_{2n}^q) \\ \vdots & \vdots & a_{ki}^q \delta(t-\tau_{ki}^q) & \vdots \\ a_{m1}^q \delta(t-\tau_{m1}^q) & a_{m2}^q \delta(t-\tau_{m2}^q) & \cdots & a_{mn}^q \delta(t-\tau_{mn}^q) \end{bmatrix} \tag{2}$$

where $\delta(\cdot)$ represents the impulse response, $a_{ki}^q$ and $\tau_{ki}^q$ are the amplitude attenuation and time delay of the $i$th source signal to the $k$th sensor through the $q$th path, respectively. To obtain the sparse characteristic of the signals, the signal $X_k(t,f)$ received by the $k$th sensor after short time Fourier transform (STFT) [18] can be written as

$$X_k(t,f) = \sum_{i=1}^{n} \sum_{q=1}^{Q} a_{ki}^q S_i^q(t-\tau_{ki}^q, f) \tag{3}$$

Take the BPSK signal as an example, the TF expression is described as

$$X_k(t,f) = \sum_{i=1}^{n} \sum_{q=1}^{Q} a_{ki}^q \widehat{h}(f \pm f_i) e^{\mp j 2\pi f_i (t-\tau_{ki}^q)} \tag{4}$$

where $f_i$ denotes the center frequency of the $i$th source signal. After performing modulus operation on $X_k(t,f)$ [19], the power $P_k(f)$ of the $k$th received signal can be expressed as

$$\begin{aligned} P_k(f) &= \int_{-\infty}^{+\infty} |X_k(t,f)| dt \\ &= \left| \sum_{i=1}^{n} \sum_{q=1}^{Q} a_{ki}^q \widehat{h}(f \pm f_i) \right| \int_{-\infty}^{+\infty} \left| e^{\mp j 2\pi f_i (t-\tau_{ki}^q)} \right| dt = \left| \sum_{i=1}^{n} \sum_{q=1}^{Q} a_{ki}^q \widehat{h}(f \pm f_i) \right| \end{aligned} \tag{5}$$

where $|\cdot|$ expresses modulus operation. When the spectrum of the source signal is non-aliased, there is only the component of the source signal $s_i(t)$ in the interval $[f_i - \Delta, f_i + \Delta]$ $(\Delta > 0)$ of the received signal. In this case, the power ratio $P_\alpha(f)/P_\beta(f)$ of any two of the received signals $\boldsymbol{X}_\alpha$ and $\boldsymbol{X}_\beta$ is

$$\begin{aligned} &P_\alpha(f)/P_\beta(f) \\ &= \frac{\left|\sum_{i=1}^{n}\sum_{q=1}^{Q} a_{\alpha i}^{q}\widehat{h}(f \pm f_i)\right|}{\left|\sum_{i=1}^{n}\sum_{q=1}^{Q} a_{\beta i}^{q}\widehat{h}(f \pm f_i)\right|} = \frac{\left|\sum_{q=1}^{Q} a_{\alpha i}^{q}\right|}{\left|\sum_{q=1}^{Q} a_{\beta i}^{q}\right|}, f \in [f_i - \Delta, f_i + \Delta] \end{aligned} \tag{6}$$

Consequently, the short-time spectral power points of the signal $s_i(t)$ will be clustered on the line with a slope of $P_\alpha(f)/P_\beta(f)$. Fig. 1 represents the scatter plot of the power ratio of the two received signals after the convolutive mixture of the four BPSK signals. Due to the sparsity of the observed signals in the power domain, the received signals exhibit linear clustering property. There are four linear clusters in Fig. 1, corresponding to the four source signals. As thus the mixed signals can be effectively separated by the traditional single-source-point (SSP) detection method [10]. However, in practical communication systems, it is almost impossible to avoid TF aliasing for communication signals. When the spectrum of the source signal is overlapped, the sparsity of the observed signals in the power domain cannot be guaranteed, thus weakening the linear clustering property of the observed signals (Fig. 2). The traditional SSP method will not accurately recover the source signal.

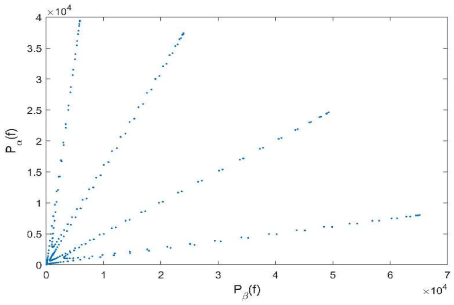


**Fig. 1** The power scatters of mixed signals

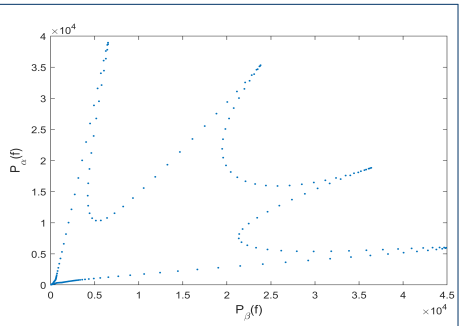


**Fig. 2** The power scatters of mixed signals with TF aliasing

## 3 The proposed method

To tackle the above challenge, we propose a new blind separation strategy based on TF soft mask. The process consists of two main stages. The first step is to determine the number of sources through the KDE algorithm followed by peak detection. After that, the contribution degree of the source signal in the observed signal is calculated by the contribution degree function to construct the TF soft mask matrix, which is used to separate the TF aliasing signals.

### 3.1 Source number estimation

In the problem of UBSS, the source number estimation is an indispensable step. The accurate estimation of the number of sources is the prerequisite for precise source signal recovery [20, 21]. In order to estimate the number of sources accurately, the KDE algorithm is used to calculate the angular probability density distribution of the mixed signal in the sparse domain followed by detecting the number of peak points of the distribution. To eliminate the interference of noise on the signal, a threshold $\varepsilon$ needs to be set to screen out the low power points. The set of frequencies $U$ after removing the low power points can be obtained by

$$U = \left\{ f \left| \sum_{k=1}^{m} P_k(f) > \varepsilon \max_f [\sum_{k=1}^{m} P_k(f)] \right. \right\} \tag{7}$$

where $\varepsilon$ is the empirical parameter, which is taken as 0.1 in this paper. In the later expressions, $f_u$ is used to denote the $u$th element of $U$. Afterwards, convert the filtered power points into angular distributions $\boldsymbol{\theta}$:

$$\theta_u = \arctan\left[P_\alpha(f_u)/P_\beta(f_u)\right] \tag{8}$$

The statistical histogram after converting to an angular distribution is shown in Fig. 3. As seen from the figure, the angular distribution is more densely distributed around the intervals 0.07, 0.52, 1.15, and 1.48 than the other intervals. Thus the angular distribution $\boldsymbol{\theta}$ is modeled based on the KDE algorithm [22]:

$$G_\kappa(\theta) = \frac{1}{l} \sum_{u=1}^{l} K_\kappa(\theta - \theta_u) \tag{9}$$

where $G_\kappa(\theta)$ denotes the angular probability density distribution of $\boldsymbol{\theta}$; $l$ is the length of the vector $\boldsymbol{\theta}$; $K_\kappa(\cdot)$ represents the kernel function with a smoothing factor $\kappa$ of the bandwidth. In this paper, we choose the Gaussian kernel as the kernel function and take $\kappa$ as 0.25.

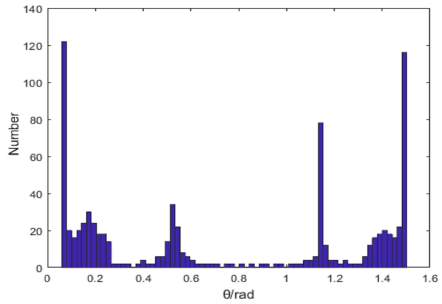


**Fig. 3** The statistical histogram of angular distribution

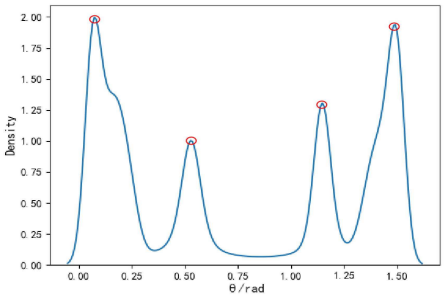


**Fig. 4** The angular probability density distribution

The angular probability density distribution obtained by the KDE algorithm is shown in Fig. 4. The number of peak points of the angular probability density

distribution is the number of sources to be estimated. As we can see from Fig. 4, there are four peak points marked by red circles, which means that the number $\widehat{n}$ of estimated source signals is four.

### 3.2 Source signal recovery by TF soft mask

Ideally, the reconstruction of the source signal is achieved by inverse short time Fourier transform (ISTFT) in the frequency band $[f_i - \Delta, f_i + \Delta]$ [10]. However, the traditional clustering method is only a kind of hard segmentation of power points to obtain the TF binary mask. When the frequency spectrum is overlapped, the short-term spectral power of the observed signals is the superposition of the short-term spectral power of the source signals. The integrity of the source signal reconstruction cannot be guaranteed through the method of hard segmentation. Thus a matching soft mask matrix $M(t, f)$ is required to fully recover the source signal.

$$Y_i(t, f) = X(t, f) \odot M_i(t, f) \tag{10}$$

where $\odot$ represents the Hadamard product; $Y_i(t, f)$ denotes the $i$th signal to be reconstructed and $M_i(t, f)$ is the corresponding TF soft mask matrix that needs to be constructed.

In this paper, the construction of the TF soft mask matrix is performed by designing a contribution degree function based on the cosine distance. It can be seen from Fig. 2 that among all the power points inside the $i$th linear cluster, the endpoint is subject to the least interference. That is, when $f_u = f_i$, the contribution degree $\eta_u^i$ of the $i$th source signal to the mixed signal can be taken as 1 and the cosine distance between the endpoint and itself is 1 as well ($f_i$ is the frequency corresponding to the endpoint of the $i$th linear clustering cluster). When $f_u$ is further away from $f_i$, the contribution degree $\eta_u^i$ will be decreased. The corresponding cosine distance $d_u^i$ between the power point and the $i$th endpoint is decreased as well. Extremely, $\eta_u^i$ is taken as 0 when $f_u$ is the frequency of the nearest adjacent endpoint. Hence the contribution degree $\eta_u^i$ can be characterized by the cosine distance between all power points and the endpoint of the $i$th linear cluster. A monotonically increasing contribution function is designed to characterize the positive correlation between contribution degree $\eta_u^i$ and cosine distance $d_u^i$:

$$\eta_u^i = \begin{cases} 1, & d_u^i = 1 \\ \left(\frac{d_u^i - d_i{}'}{1 - d_i{}'}\right)^{\gamma}, & 0 < d_u^i < d_i{}' \\ 0, & otherwise \end{cases} \tag{11}$$

where $d_i{}'$ denotes the maximum of the cosine distance between the endpoint of the $i$th linear cluster and the endpoints of the remaining linear clusters; $\gamma$ denotes the scaling factor of the contribution function, whose different values will affect the separation performance of the algorithm. In section 4.1 we will discuss the impact of $\gamma$ on separation performance. The cosine distance $d_u^i$ of the $u$th power point from the endpoint of the $i$th linear cluster is obtained as

$$d_u^i = CD\left\{\left[\begin{array}{cc} P_\alpha(f_i), & P_\beta(f_i) \end{array}\right], \left[\begin{array}{cc} P_\alpha(f_u), & P_\beta(f_u) \end{array}\right]\right\} \tag{12}$$

where $CD$ denotes the cosine distance between two points. The frequencies corresponding to the endpoints of the clustering clusters can be detected by seeking the first $\widehat{n}$ peak points in the sum of the power data marked in red Fig. 5. The points marked in red are the endpoints of the detected linear clusters to be determined in Fig. 6. Therefore, the contribution degree of the $u$th point to the $i$th linear cluster can be calculated by the contribution degree function given above.

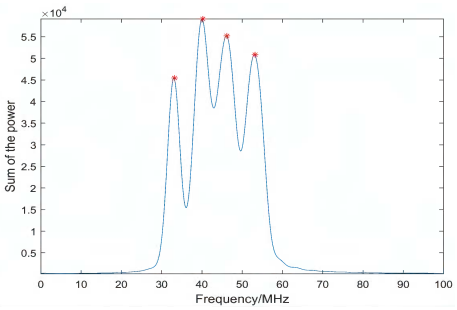


**Fig. 5** The sum of the power data

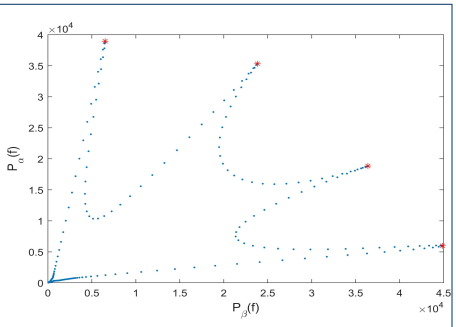


**Fig. 6** The power scatters of mixed signals after detecting

Based on the contribution degree $\eta_u^i$ obtained from Eq. (11), the $i$th TF soft mask matrix $\boldsymbol{M}_i$ is constructed by the following formula:

$$\boldsymbol{M}_i = \begin{bmatrix} \eta_1^i & \eta_2^i & \cdots & \eta_F^i \\ \eta_1^i & \eta_2^i & \cdots & \eta_F^i \\ \vdots & \vdots & \ddots & \vdots \\ \eta_1^i & \eta_2^i & \cdots & \eta_F^i \end{bmatrix}_{T\times F} \tag{13}$$

where $F$ is the number of STFT frequencies; $T$ is the number of time series of STFT. $\widehat{n}$ soft mask matrices can be constructed in this way.

The $i$th source signal $y_i(t)$ to be reconstructed is

$$y_i(t) = ISTFT\left[X(t,f) \odot M_i(t,f)\right] \tag{14}$$

where $X(t,f)$ indicates the sum of the observed signals.

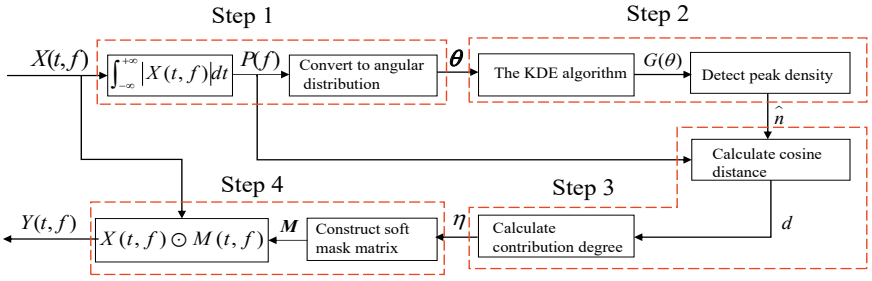


**Fig. 7** The flowchart of the proposed method

The flowchart of the proposed strategy is shown in Fig. 7. Firstly, the angular distribution $\boldsymbol{\theta}$ is converted from the power ratio by Eq. (8); Secondly, the number $\widehat{n}$ of source signals is estimated through the KDE algorithm followed by the peak density detection; Afterwards, the contribution degree $\eta$ of the source signal in the observed signal is calculated by the contribution degree function based on the cosine distance $d$. Finally, the TF soft mask matrix $\boldsymbol{M}$ is constructed based on the contribution degree $\eta$ and the separated TF signals are reconstructed.

## 4 Simulation results and discussion

Our simulations are aimed at investigating the anti-aliasing performance and anti-noise performance of the proposed algorithm. To measure the degree of spectrum aliasing of the source signals, we define the degree of spectrum aliasing $\lambda$:

$$\lambda = \frac{B_o}{B} \times 100\% \tag{15}$$

where $B$ represents the source signal spectrum bandwidth, $B_o$ represents the maximum aliasing width between the source signal spectrum and the adjacent signal spectrum.

Since the "boundary effect" of STFT has an impact on the separation performance [10], we selected the Kaiser window ($\beta = 6.865$) as the window function. The evaluation criteria of separation performance were applied in our simulations, which include the source to distortion ratio (SDR), the source to interferences ratio (SIR), the source to artifacts ratio (SAR) [23], and the separated bit error rate (BER). To obtain bitstream information, the coherent demodulation method was used to demodulate the separated source signals. The mixed signals were separated by the SCA algorithm proposed in this paper and the literature [8][10]. The benchmark algorithm in [8] belonged to the classic two-stage method, and [10] used the TF masking method to separate the source signal.

### 4.1 Simulation 1: The selection of scaling factor of the contribution degree function

In this simulation experiment, we verified the impact of the scaling factor on the separation performance of the proposed algorithm. The simulation was conducted under the condition of additive white Gaussian noise with a signal-to-noise ratio (SNR) of 16.4 dB. It is assumed that the three signals with different modulation (2ASK/BPSK/QPSK) are mixed instantaneously, in which the symbol rate of the signals are $5 \times 10^6$, $5 \times 10^6$, $10 \times 10^6$ B, respectively. The modulation carrier frequencies are 13.5, 20, 26.5 MHz, respectively, with the $\lambda$ of each signal being 35%. The mixing matrix $\boldsymbol{A}$ is

$$\boldsymbol{A} = \begin{bmatrix} 0.21 & 0.63 & 0.89 \\ 0.92 & 0.58 & 0.22 \end{bmatrix} \tag{16}$$

The separation performance with different $\gamma$ is shown in Fig. 8, the bigger value is, the better the separation performance is. It can be seen that, with $\gamma$ increasing, the SIR decreased significantly while the SAR and SDR remain almost constant. Thus we take $\gamma$ as 0.5 in the following simulation experiments. Fig. 9 and Fig. 10 show the

waveforms of the source signals and their mixed signals respectively. Comparatively, Fig. 11 shows the waveforms of the signals separated by the proposed algorithm with $\gamma = 0.5$. It can be seen that the waveforms of the separated signals are basically consistent with the source signals. Although the waveforms have some distortion at the junction of 0 and 1 bits, which is caused by the "boundary effect" of STFT, it does not affect the subsequent demodulation and judgment. Fig. 12 represents the waveforms after coherent demodulation. The bit data can be recovered by setting the appropriate judgment level.

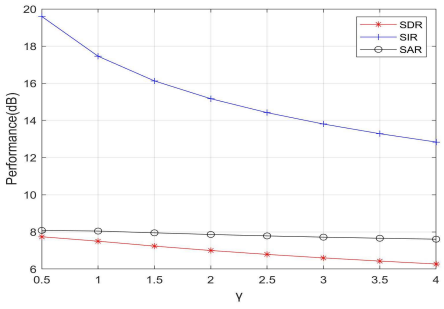


**Fig. 8** The separation performance with different $\gamma$

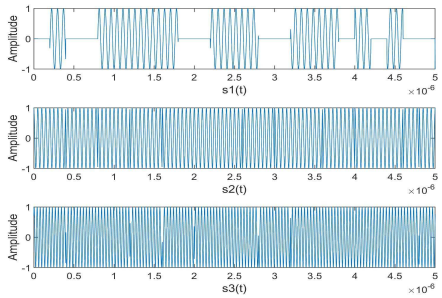


**Fig. 9** The waveforms of source signals

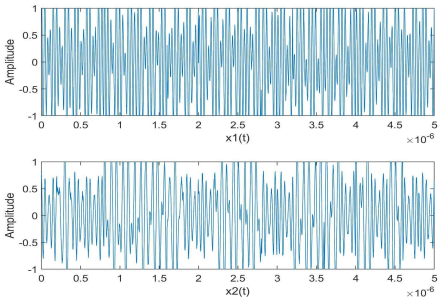


**Fig. 10** The waveforms of mixed signals

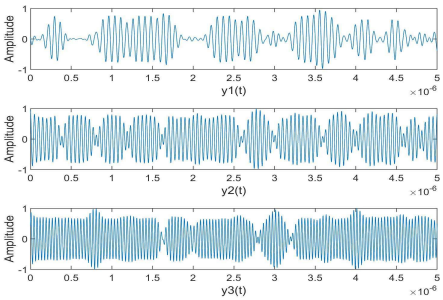


**Fig. 11** The waveforms of separated signals

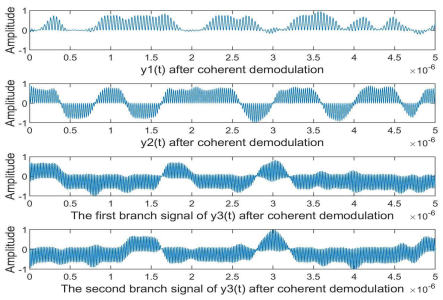


**Fig. 12** The waveforms of separated signals after coherent demodulation

### 4.2 Simulation 2: The anti-aliasing performance simulation

To analyze the anti-aliasing performance for signals with different modulation methods, two sets of signals were used as the source signals, which respectively were three signals with the same BPSK modulation and three signals with different modulation (2ASK/BPSK/QPSK). The symbol rate of a single source signal is $5 \times 10^6$ B. The modulation carrier frequencies were designed according to different $\lambda$. In this simulation, it is assumed that the source signals propagate in two channels before being received by the sensors and the SNR is 15 dB. The first channel of signals arrived instantaneously, and the corresponding mixing matrix is

$$\boldsymbol{A}_1 = \begin{bmatrix} 0.23 & 0.32 & 0.52 \\ 0.44 & 0.47 & 0.13 \end{bmatrix} \tag{17}$$

The second channel of signals arrived with delay, the signal propagation delay matrix and the corresponding mixing matrix are

$$\boldsymbol{T} = \begin{bmatrix} 0.1 & 0.05 & 0.2 \\ 0.18 & 0.1 & 0.04 \end{bmatrix} \tag{18}$$

$$\boldsymbol{A}_2 = \begin{bmatrix} 0.22 & 0.42 & 0.37 \\ 0.41 & 0.17 & 0.28 \end{bmatrix} \tag{19}$$

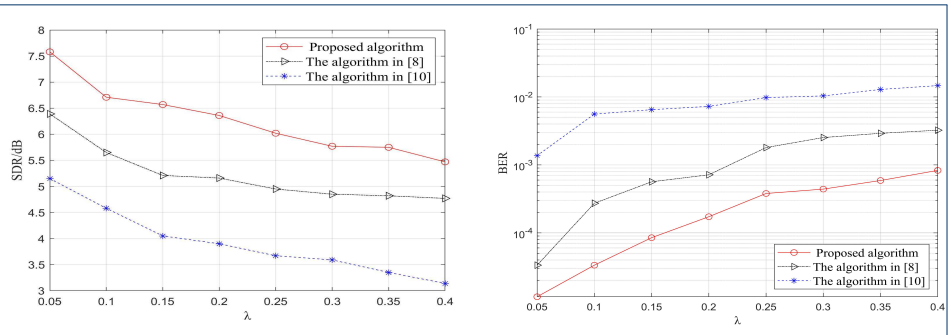


**Fig. 13** The separation performance of three BPSK signals with different $\lambda$

The SDR and BER of the separated signals with the increase of the $\lambda$ are shown in Fig. 13 and Fig. 14 (the left figure represents the SDR, and the right represents the BER). From the simulation results, it can be seen that in the environment with the SNR of 15 dB, as the source signal spectrum aliasing gradually intensifies, the separation performance of the proposed algorithm and the benchmark algorithms are reduced to varying degrees. However, for signals with the same BPSK modulation (Fig. 13), the average of the separated signals by the proposed algorithm is increased by 1.05 and 2.35 dB compared with the comparison algorithms. For signals with different modulation (Fig. 14), the average of the separated signals by the proposed algorithm is increased by 0.68 and 2.48 dB. The BER is significantly lower than that by the comparison algorithms. As a result, the anti-aliasing performance of the algorithm in this paper is more excellent.

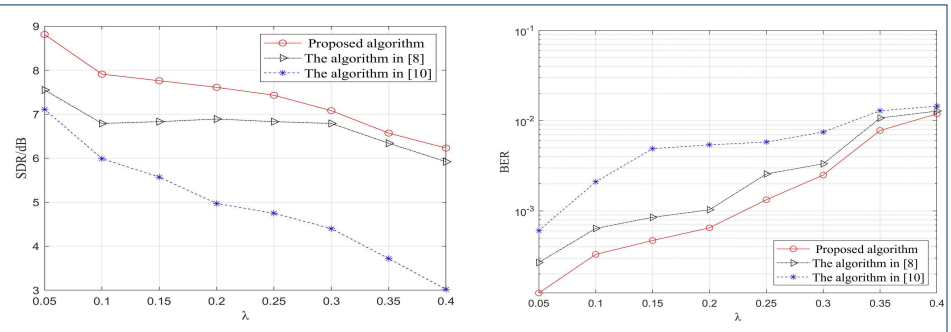


**a** **b**

**Fig. 14** The separation performance of different modulation signals with different $\lambda$

### 4.3 Simulation 3: Simulation of algorithm anti-noise performance

In this simulation, the carrier frequency of each of the 2 groups of source signals was set to 14 MHz, 20 MHz, and 26 MHz, and the was fixed at 40% correspondingly. In the environment of the SNR from 5 to 30 dB, the method in simulation 2 was used to mix the source signals. The SDR and BER of the separated signals with the increase of the SNR are shown in Fig. 15 and Fig. 16:

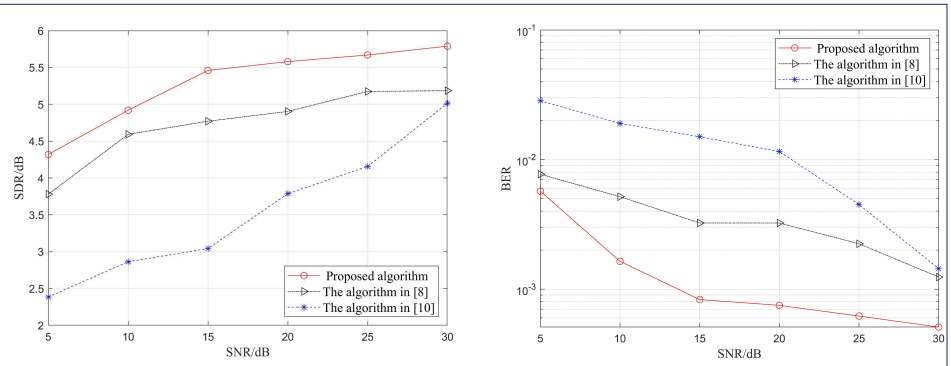


**a** **b**

**Fig. 15** The separation performance of three BPSK signals under different SNR

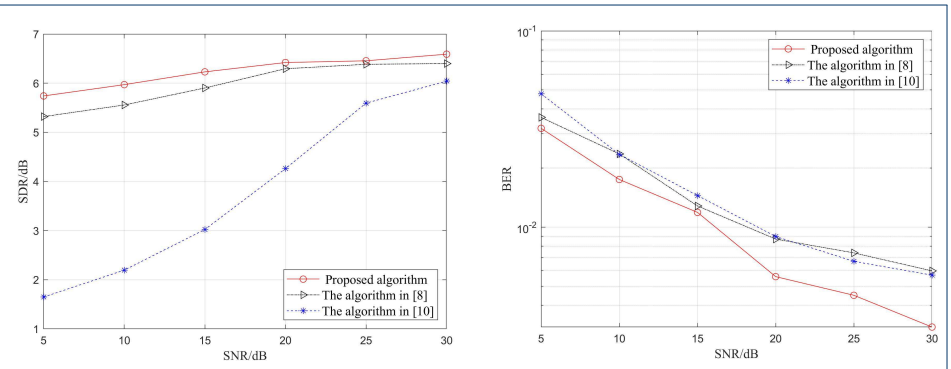


**a** **b**

**Fig. 16** The separation performance of different modulation signals under different SNR

It can be seen from figures that, with the SNR increases, the separation performance of the algorithm proposed in this paper and the benchmark algorithms have been effectively improved. However, compared with the benchmark algorithms, the SDR and BER of the separated signals by the proposed algorithm is higher and lower respectively, indicating that the signal separation performance is better. Especially for signals with the same BPSK modulation (Fig. 15), when , the BER of the separated signals is lower than 10-2. For signals with different modulation (Fig. 16), the BER drops below 10-2 when the SNR reaches 20.

## 5 Conclusions

In this article, we have discussed an underdetermined mixed blind signal separation method with the application of TF overlapped communication signals. A novel blind signal separation algorithm based on the TF soft mask matrix is studied. In the proposed method, we utilize the KDE algorithm to obtain the angle probability density distribution, followed by which the source number is estimated by detecting the peak points of the distribution. Then the contribution degree function is designed to generate the contribution degree, based on which the TF soft mask matrix is constructed to obtain the reconstructed TF signal. This method enables to overcome the poor performance of blind separation for TF aliasing communication signals by traditional separation algorithms. The algorithm's anti-aliasing ability and anti-noise ability are simulated and verified by simulation.

**Abbreviations**

TF: Time-frequency; KDE: Kernel density estimation; BSS: Blind source separation; ICA: Independent component analysis; UBSS: Underdetermined blind source separation; SCA: Sparse component analysis; STFT: Short time Fourier transform; SSP: Single-source-point; ISTFT: Inverse short time Fourier transform; SDR: Distortion ratio; SIR: Source to interferences ratio; SAR: Source to artifacts ratio; BER: Bit error rate; SNR: signal-to-noise ratio.

**Acknowledgements**

The authors would like to thank the anonymous reviewers and the editors for helping improve this work.

**Authors' contributions**

HM participated in the design of the study, performed the simulation analysis and drafting the manuscript. XZ, XW, LY and YZ participated in the English correction and integration of the paper. All authors read and approved the fnal manuscript.

**Funding**

Not applicable.

**Availability of data and materials**

The data used in this article are all randomly generated using Matlab software.

**Competing interests**

The authors declare that they have no competing interests.

**Author details**

School of Communication Engineering, Army Engineering University, Nanjing, China.

**References**

1. C. Wei, H. Peng, J.H. Fan, A Blind Separation Method of PCMA Signals Based on MSGibbs Algorithm. Journal of Physics: Conference Series,IOP Publishing. **1168**(5), 052050 (2019)
2. W. Miao, C. Xiao-xia, Z. Ke-fan, A Blind Separation of Variable Speed Frequency Hopping Signals based on Independent Component Analysis. In 2019 IEEE 3rd Information Technology, Networking, Electronic and Automation Control Conference (ITNEC). 144–148 (2019). https://doi.org/10.1109/ITNEC.2019.8729324
3. R. Sharma, Musical Instrument Sound Signal Separation from Mixture using DWT and Fast ICA Based Algorithm in Noisy Environment. Materials Today: Proceedings. **29**, 536–547 (2020)
4. S. Ziani, A. Jbari, L. Bellarbi, Y. Farhaoui, Blind maternal-fetal ECG separation based on the time-scale image TSI and SVD-ICA methods. Procedia computer science. **134**, 322–327 (2018)
5. Z. Luo, C. Li, L. Zhu, A comprehensive survey on blind source separation for wireless adaptive processing: Principles, perspectives, challenges and new research directions. IEEE Access. **6**, 66685–66708 (2018)

6. B. Ma, T. Zhang, Single-channel blind source separation for vibration signals based on TVF-EMD and improved SCA. IET Signal Processing. **14**(4), 259–268 (2020)
7. L. Zhen, et al, Underdetermined blind source separation using sparse coding. IEEE transactions on neural networks and learning systems. **28**(12), 3102–3108 (2016)
8. B. Fang, G. Huang, J. Gao, Underdetermined blind source separation for LFM radar signal based on compressive sensing. In?2013 25th Chinese Control and Decision Conference (CCDC), IEEE. 1878–1882 (2013)
9. W. Fu, J. Chen, Y. Bo, Source recovery of underdetermined blind source separation based on SCMP algorithm. IET Signal Processing. **11**(7), 877–883 (2017)
10. G. Yu, Underdetermined Blind Source Separation Method with Application to Modal Identification. Shock and Vibration. **2019**, (2019)
11. M. Cobos, J.J. Lopez, Maximum a posteriori binary mask estimation for underdetermined source separation using smoothed posteriors. IEEE transactions on audio, speech, and language processing. **20**(7), 2059–2064 (2012)
12. M. Kumar, V. E. Jayanthi, Underdetermined blind source separation using CapsNet. Soft Computing. **24**(12), 9011–9019 (2020)
13. Y. Li, W. Nie, F. Ye, Y. Lin, A mixing matrix estimation algorithm for underdetermined blind source separation. Circuits, Systems, and Signal Processing. **35**(9), 3367–3379 (2016)
14. Y. Liu, L. Li, D. Lv, N. Pan, Novel source recovery method of underdetermined time-frequency overlapped signals based on submatrix transformation and multi-source point compensation. IEEE Access. **7**,29610–29622 (2019)
15. V. G. Reju, S. N. Koh, Y. Soon, Underdetermined convolutive blind source separation via time-frequency masking. IEEE Transactions on Audio, Speech, and Language Processing. **18**(1), 101–116 (2009)
16. A. M. Reddy, B. Raj, Soft mask methods for single-channel speaker separation. IEEE Transactions on Audio, Speech, and Language Processing. **15**(6), 1766–1776 (2007)
17. T. Duan, X. Zhang, A solution to blind separation of convolutive communication mixtures in frequency domain. In?2012 2nd International Conference on Consumer Electronics, Communications and Networks (CECNet), IEEE. 2330–2333 (2012)
18. B. Ma, et al, A blind source separation method for time-delayed mixtures in underdetermined case and its application in modal identification. Digital Signal Processing. **112**,103007 (2021)
19. C. Li, L. Zhu, Z. Luo, Underdetermined blind source separation of adjacent satellite interference based on sparseness. China communications. **14**(4), 140–149 (2017)
20. J. Lu, W. Cheng, D. He, Y. Zi, A novel underdetermined blind source separation method with noise and unknown source number. Journal of Sound and Vibration. **457**,67–91 (2019)
21. J. E. Ozbek, Determining the Number of Sources with Diagonal Unloading in Single-Channel Mixtures. Circuits, Systems, and Signal Processing. **40**,5483–5499 (2021)
22. S. Weglarczyk, Kernel density estimation and its application. In ITM Web of Conferences. **23**,00037 (2018)
23. E. Vincent, et al, Performance measurement in blind audio source separation. IEEE transactions on audio, speech, and language processing. **14**(4), 1462–1469 (2006)